International Journal of Heat and Mass Transfer 52 (2009) 4986–4996

Contents lists available at ScienceDirect

International Journal of Heat and Mass Transfer

journal homepage: www.elsevier.com/locate/ijhmt

Transient temperature profile inside thermoacoustic refrigerators

Pierrick Lotton [a,*], Philippe Blanc-Benon [b], Michel Bruneau [a], Vitaly Gusev [c], Serge Duffourd [b], Mikhail Mironov [d], Gaelle Poignand [b]

[a] Laboratoire d'Acoustique de l'Université du Maine, UMR CNRS 6613, 72 085 Le Mans cedex 9, France
[b] Laboratoire de Mécanique des Fluides et d'Acoustique, UMR CNRS 5509, Ecole Centrale de Lyon, France
[c] Laboratoire de Physique de l'Etat Condensé, UMR CNRS 6807, Université du Maine, 72 085 Le Mans cedex 9, France
[d] Andreev Acoustics Institute, Russian Academy of Sciences, Moscow, Russia

ARTICLE INFO

Article history:
Received 21 April 2008
Received in revised form 7 January 2009
Accepted 9 March 2009
Available online 1 July 2009

Keywords:
Thermoacoustics
Transient response

ABSTRACT

The linear theory used to calculate the thermal quantities inside the stack in the classical thermoacoustic refrigerators always overestimates those measured. The causes of these discrepancies have to be found in the complex processes of thermal exchanges. The analytical study of the transient response should provide an interpretation of these complex processes. This present paper provides such analytical modelling. This modelling remains within the framework of the classical linear theory. It includes the effects of the thermoacoustic heat flux carried along the stack, the conductive heat flux returning in the solid walls of the stack and through the fluid inside the stack, the transverse heat conduction in the stack and the heat leakages through the duct walls, the heat generated by viscous losses in the stack, the heat generated by vorticity at the ends of the stack, and the heat transfer through both ends of the stack. A modal analytical solution for the temperature profile is proposed, assuming the usual approximations in such thermal problems to avoid intricate calculations and expressions. The theoretical transient response of a thermoacoustic refrigerator is compared with experimental data. A good qualitative agreement is obtained between analytical and experimental results after fitting empirical coefficients.

1. Introduction

In the classical design of thermoacoustic refrigerators, a stack of parallel plates (or any other equivalent porous material) is set in an acoustic resonator. Thermoacoustic process occurs inside the stack of plates when subjected to an acoustic wave. This acoustic wave induces thermal interactions between gas and plates leading to a hydrodynamical non-zero time-average heat transfer along the plates. This heat flow induces a temperature gradient along the stack. When permanent regime is reached, a stationary temperature difference ΔT is obtained between the ends of the stack.

The behaviour of a thermoacoustic refrigerator can be described by using the linear steady state theory [1], assuming a balance between the thermoacoustic heat flux carried along the stack and the conductive heat flux returning through both the solid walls of the stack and the fluid inside the stack. This steady state assumption gives quite reasonable results for the estimation of refrigerator performance values such as temperature difference, heat flow extracted from the cold heat exchanger or coefficient of performance (COP). Therefore, the quasi-steady assumption is widely used. However, some transient phenomena, which occur during "on–off" operations or after variations of operating conditions (thermal load variations, adjustment of resonance frequency [2], etc.), may be interesting and important. These phenomena, related to dynamic behaviour, require today greater interest, especially when designing thermoacoustic refrigerators, as for other refrigeration devices [3,4]. Few experimental and numerical data on the transient process in a thermoacoustic refrigerator exist in the literature [5–10]. In particular, a simplified model has been developed to calculate the transient temperature gradient in a short stack [9] and transient effects have been addressed using narrow duct approximation, both aiming at interpreting theoretically the singularity in the mean temperature at the closed end of the tube [10]. But an analytical global modelling of the heat transfers during the transient regime in a thermoacoustic refrigerator is still not reported.

Besides that, transient processes have been studied in thermoacoustic standing wave [11–15] and travelling wave [16,17] prime movers. Complex transient behaviours due to non-linear phenomena have been enlightened, as periodic turn on and turn off regimes [11,17] or double threshold phenomena [16]. Coupling such a thermoacoustic prime mover with a thermoacoustic refrigerator would probably lead to more complicated transient behaviours. Thus, the study of transients in thermoacoustic refrigerators is essential for interpreting these expected complex behaviours.

Returning to the thermoacoustic refrigerator itself, the temperature difference ΔT calculated in the framework of the steady state

* Corresponding author. Tel.: +33 243 833 770; fax: +33 243 833 520.
E-mail address: pierrick.lotton@univ-lemans.fr (P. Lotton).

0017-9310/$ - see front matter © 2009 Elsevier Ltd. All rights reserved.
doi:10.1016/j.ijheatmasstransfer.2009.03.075

Nomenclature

c_0	adiabatic speed of sound
$C_m(t)$	coefficient defined in Eq. (28b)
C_p	fluid specific heat at constant pressure
C_s	stack material specific heat coefficient
C_v	fluid specific heat coefficient at constant volume
e_s	stack plate half thickness
f	frequency
$f_m(t)$	coefficient defined in Eq. (30b)
$g(x)$	function defined in Eq. (15)
h_{e0}	heat transfer coefficient
$h_{e\ell}$	heat transfer coefficient
h_L	heat exchange coefficient ($W\,m^{-2}\,K^{-1}$)
i	$\sqrt{-1}$
k	wave number
K	fluid thermal conductivity
K_{eq}	effective thermal conductivity in the stack region
k_m	eigen value
K_s	stack material thermal conductivity
ℓ	stack length
$L + x_0$	resonator length
p	acoustic pressure
P_0	atmospheric pressure
$q(x)$	function defined in Eq. (6)
Q_c	conductive heat flux
q_ℓ	coefficient defined in Eq. (24c)
Q_L	heat leakages through the resonator wall
Q_{th}	thermoacoustic hydrodynamical heat flux
q_0	coefficient defined in Eq. (24b)
q_v	coefficient defined in Eq. (17)
Q_v	heat generated by viscous losses
Q_{vort}	heat flux due to vorticity at the ends of the stack
$r(x)$	thermoacoustically induced thermal conductivity
S	resonator section area
u_x	axial component of particle velocity
s	entropy variation per unit mass
S_L	form factor defined in Eq. (13)
t	time
T_m	local time-averaged temperature
T_∞	ambiant temperature outside the resonator
V	stack volume
v_x	real part of axial component of particle velocity
x	longitudinal coordinate
x_c	distance between loudspeaker and stack centre
x_0	distance between loudspeaker and stack entrance
x_s	stack centre coordinate
y_0	fluid layer half thickness

Greek symbols

α	coefficient defined in Eq. (24a)
β	coefficient defined in Eq. (24a)
γ	$\frac{C_p}{C_v}$
δ_v	viscous penetration depth
δ_h	thermal penetration depth
ΔT	temperature difference between stack ends
ζ_L	coefficient defined in Eq. (16)
η_0	coefficient defined in Eq. (24b)
η_ℓ	coefficient defined in Eq. (24c)
$\theta(x,t) = T_m - T_\infty$	temperature difference
μ	shear viscosity coefficient
ξ	variable defined in Eq. (19)
ρ'	fluid density variation
ρ_0	fluid mean density
ρ_S	stack material density
σ	Prandtl number
τ	temperature variation
$\varphi(x)$	initial temperature spatial distribution
χ_T	isothermal compressibility
ψ_m	eigen function
ω	angular frequency

Subscripts

h	thermal
m	eigenfunction expansion
s	stack
v	viscous

linear theory generally overestimates the measured one at high drive ratio DR (ratio of the acoustic pressure amplitude p_0 to the mean pressure P_0) [18–21]. Whilst the measurements of ΔT agree quite well with the theory for drive ratios less than approximately 0.2% (the deviation is lower than 25%) [9], the predicted ΔT value overestimates the measured one and the discrepancy increases at increasing drive ratios (discrepancies up to 300% are reported for drive ratios greater than 1%) [21].

The reliability of the theoretical results obtained using the linear theory suffers from intrinsic limitations which can be due to the following causes: non-linear acoustic effects (harmonic generation, acoustic streaming), turbulent flow, vortex generation and jetting (which occur at the stack ends), heat leakages through the duct walls, heat generated by viscous losses in the stack, heat transfer through the end of the stack, non-linear distortion of the temperature oscillations inside the stack. Then works have been carried out in order to both investigate the origin of the deviation of the predictions from the linear theory against the measured performance of real devices and also to address the requirements that have to be taken into account in the design of thermoacoustic refrigerators (because each effect can play an important role in the efficiency of the devices) [6–8,20,22–28]. But heat transfer phenomena appear to be more critical than non-linear acoustic or non-linear thermal phenomena in determining the overestimation that theoretical predictions make on experimental values of the temperature gradient. The causes of these discrepancies have to be found in the complex processes of thermal exchanges. Thus, a global modelling of the heat transfers during the transient regime (up to the stationary regime) should bring important information concerning these discrepancies in steady state regime.

The aim of this paper is to provide a first step in the derivation of such a global analytical modelling. This modelling remains within the framework of the classical linear theory. It includes the effects of the thermoacoustic heat flux carried along the stack, the conductive heat flux returning in the solid walls of the stack and through the fluid inside the stack, the transverse heat conduction in the stack and the heat leakages through the duct walls, the heat generated by viscous losses in the stack, the heat generated by vorticity at the ends of the stack, and the heat transfer through both ends of the stack (with or without heat exchangers). These thermal mechanisms are detailed in the first part of this paper. A modal analytical solution for the temperature profile is then developed in a second part, assuming the usual approximations in such thermal problems to avoid intricate calculations and expressions. This modelling explains not only the temperature difference ΔT between both ends of the stack, but also the temperature at any loca-

tion inside the stack as a function of time. In a third part, the experimental transient response of a thermoacoustic refrigerator is presented and compared with theoretical one.

2. The thermal mechanisms involved inside and around the stack: the basic equations for the temperature profile

The thermoacoustic device considered in this study is schematically represented in Fig. 1. It comprises an acoustic source (an electrodynamic loudspeaker) coupled to a closed cylindrical (section area S, length $L+x_0$) waveguide in which is set a stack of plates. The thickness of each plate of the stack is denoted $2e_s$, the thickness of the fluid layer between the plates of the stack is denoted $2y_0$. The axial coordinates of the ends of the stack are denoted $x=0$ and $x=\ell$, the coordinate x_s of the centre of the stack being determined by $x_s=\ell/2$. The centre of the stack is also defined by its distance from the loudspeaker $x_c=x_0+x_s$. Heat exchangers are set close to the ends of the stack. Thermoacoustic cavity can be described in three parts. Two of them are "large" cylindrical tubes, one extending from the loudspeaker to the entrance of the stack and the other one from the output of the stack to the closed end of the resonator. These are separated by the stack region $(x\in(0,\ell))$.

The behaviour of the thermoviscous fluid oscillating around the steady state is described by a set of thermodynamical variables, mainly the pressure variation p, the particle velocity u_x in the axial direction, the density variation ρ', the entropy variation per unit mass s and the temperature variation τ, all of which are assumed to be small so that linear approximation remains valid. The thermostatic state and the nature of the fluid are then accounted for, respectively, by thermostatic parameters and by phenomenological quantities, respectively, such as: the ambient values P_0 of the pressure and ρ_0 of the density, the local time-averaged temperature T_m (which depends on the coordinate x and on the time), the adiabatic speed of sound c_0, the shear viscosity coefficient μ, the diffusive thermal conductivity of the fluid K, the Prandtl number σ, the heat coefficients at constant pressure and constant volume per unit of mass C_p and C_v, their ratio $\gamma=\frac{C_p}{C_v}$ and the isothermal compressibility χ_T. The plates of the stack are described by their density ρ_s, their specific heat per unit of mass C_s and their diffusive thermal conductivity K_s. The viscous penetration depth δ_v and the thermal penetration depth δ_h in the fluid are given, respectively, by

$$\delta_v=\sqrt{\frac{2\mu}{\rho_0\omega}} \tag{1}$$

and

$$\delta_h=\sqrt{\frac{2K}{\rho_0 C_p\omega}}. \tag{2}$$

The angular frequency of the harmonic signal is denoted ω and the associated period is denoted T.

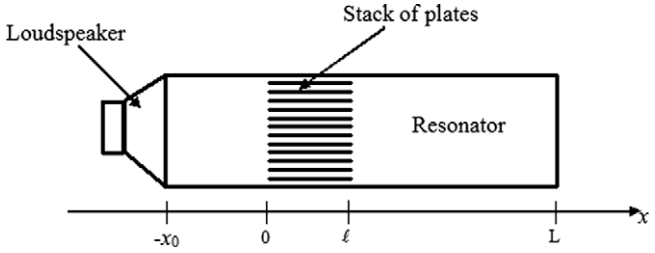

Fig. 1. Schematic view of a cylindrical thermoacoustic refrigerator.

The fluid considered is Stokesian (stress proportional to rate of strain and heat flux proportional to temperature gradient), homogeneous and at rest. The acoustic movement is assumed to be linear. Given the specificity of the aim of this paper, the correction of the length of the resonator due to coupling with the acoustic source [29] is not included below. Then, assuming that the stack does not perturb the standing wave appreciably, the acoustic pressure can be written (the time factor $\exp(i\omega t)$ is omitted)

$$p(x)=p_0\cos k(x+x_0), \tag{3}$$

where x_0 denotes the position of the loudspeaker and where $k=\omega/c_0$. The x-component $u_x(x,y)$ of the particle velocity between two plates of the stack, function of the acoustic pressure gradient, is given by [1],

$$u_x(x,y)=\frac{i}{\rho_0\omega}\left(\frac{y_0}{y_0+e_s}\right)^{-1}\frac{\partial p(x)}{\partial x}\times\left(1-\frac{\cosh[(1+i)y/\delta_v]}{\cosh[(1+i)y_0/\delta_v]}\right), \tag{4}$$

where the ratio $y_0/(y_0+e_s)$ is the porosity of the stack. The important physical phenomena involved in the process inside the stack considered here can be described as the combined effects of heat fluxes. It is namely the superposition of four kinds of heat transfer phenomena: the hydrodynamic heat flux due to thermoacoustic effect, the heat leakages through the lateral duct wall, the heat generated by viscous losses inside the stack and the conductive heat flux returning in the solid walls of the stack and along the fluid inside the stack. These heat transfer phenomena are expressed below, assuming the usual approximations in linear thermoacoustic theory [30,31] (quasi-plane wave approximation, short stack approximation, working gas assumed to be an ideal gas, no temperature dependance of the thermo-physical properties of the fluid and the plates, large heat capacity per unit area of the plates, time-averaged temperature of the plates at any coordinate x inside the stack equal to the time-averaged temperature of the gas T_m at the same coordinate):

(i) the hydrodynamic heat flux (time average over an acoustic period) due to the thermoacoustic effect [1], creating a temperature gradient along the stack, given per unit area by

$$Q_{th}(x,t)=q(x)-r(x)\frac{\partial\theta(x,t)}{\partial x}, \tag{5}$$

where $\theta(x,t)=T_m-T_\infty$ is the temperature difference between the mean temperature T_m inside the stack and T_∞ the ambient temperature outside the resonator, with

$$q(x)=\frac{-\delta_h}{2y_0}\frac{p_0^2}{\rho_0c_0}\left(1+\frac{e_s}{y_0}\right)\cos k(x+x_0)\sin k(x+x_0)\times\frac{(1+\sqrt{\sigma}-\delta_v/y_0)\alpha T_m}{(1+\sigma)\sqrt{1-\delta_v/y_0+\delta_v^2/(2y_0^2)}} \tag{6}$$

assuming that $(\alpha T_m\cong 1)$ does not depend significantly on the time in the expression $q(x)$, and with

$$r(x)=\frac{\delta_h}{2y_0}\frac{p_0^2}{\rho_0c_0}\left(1+\frac{e_s}{y_0}\right)^2\frac{C_P}{c_0\omega}\frac{1-\sigma\sqrt{\sigma}}{1-\sigma^2}sin^2k(x+x_0), \tag{7}$$

$r(x)$ being the so-called thermoacoustically induced thermal conductivity,

(ii) the heat leakages through the lateral duct wall, per unit area and per unit time, given by [30,31],

$$Q_L=-h_L\theta(x), \tag{8}$$

where h_L denotes an empirical "heat exchange coefficient" $(\mathrm{W\,m^{-2}\,K^{-1}})$,

(iii) the heat generated by viscous losses inside the stack, per unit volume, defined as

$$Q_v = \frac{1}{y_0}\int_0^{y_0}\frac{1}{T}\int_0^{T}\mu\left(\frac{\partial v_x(x,y,t)}{\partial y}\right)^2 dt\,dy, \tag{9}$$

v_x being the real part of u_x, which gives straightforwardly after a lengthy calculation, invoking solution (4) for the particle velocity,

$$Q_v = \frac{\mu}{4y_0\delta_v}\frac{p_0^2}{\rho_0^2 c_0^2}\left(1+\frac{e_s}{y_0}\right)^2\frac{\sinh(2y_0/\delta_v)-\sin(2y_0/\delta_v)}{|\cosh[(1+i)y_0/\delta_v]|^2}\sin^2 k(x+x_0), \tag{10}$$

(iv) the conductive heat flux returning in the solid walls of the stack and along the fluid inside the stack, per unit area,

$$Q_c = -K_{eq}\frac{\partial\theta}{\partial x}, \tag{11}$$

where

$$K_{eq} = \frac{(2y_0K + 2e_sK_s)}{2(y_0+e_s)} \tag{12}$$

is the effective thermal conductivity in the stack region. Then, considering an element of the stack of length dx, the energy balance is governed by the following heat diffusion equation, in the interval $x \in (0,\ell)$:

$$2(y_0\rho_0C_p + e_s\rho_sC_s)\frac{\partial\theta}{\partial t} = 2(y_0+e_s)\left(-\frac{\partial Q_{th}}{\partial x}-\frac{\partial Q_c}{\partial x}+Q_v+S_LQ_L\right), \tag{13}$$

where $S_L = S/V$ with S the section area of the stack and V the volume of the stack. In the analytical model developed by [9], it can be noted that the factors Q_v and Q_L are not introduced by the authors for interpreting the transient behaviour of the temperature, therefore the characteristic time for stabilisation of the temperature cannot be interpreted.

Invoking Eqs. (5)–(11) in Eq. (13) gives

$$\frac{\partial\theta}{\partial t} = \frac{2(y_0+e_s)}{2(y_0\rho_0C_p+e_s\rho_sC_s)} \times\left[(K_{eq}+r(x))\frac{\partial^2\theta}{\partial x^2}+\frac{\partial r(x)}{\partial x}\frac{\partial\theta}{\partial x}-S_Lh_L\theta+\left(Q_v-\frac{\partial q(x)}{\partial x}\right)\right]. \tag{14}$$

Introducing the function

$$g(x) = \frac{2(y_0+e_s)}{2(y_0\rho_0C_p+e_s\rho_sC_s)}(K_{eq}+r(x)), \tag{15}$$

and the following notations

$$\zeta_L = \frac{2(y_0+e_s)}{2(y_0\rho_0C_p+e_s\rho_sC_s)}S_Lh_L, \tag{16}$$

$$q_v = \frac{2(y_0+e_s)}{2(y_0\rho_0C_p+e_s\rho_sC_s)}\left(Q_v-\frac{\partial q(x)}{\partial x}\right), \tag{17}$$

allows Eq. (14) to be re-written as follows:

$$\frac{\partial\theta}{\partial t} = \frac{\partial}{\partial x}\left[g(x)\frac{\partial\theta}{\partial x}\right]-\zeta_L\theta+q_v. \tag{18}$$

Considering the new variable

$$\xi = \int_0^x\frac{g(0)}{g(u)}du \tag{19}$$

gives

$$\frac{\partial}{\partial x}\left[g(x)\frac{\partial\theta}{\partial x}\right] = \frac{g^2(0)}{g(x)}\frac{\partial^2\theta}{\partial\xi^2}, \tag{20}$$

and then, assuming that $g(x)$ does not depend significantly on the spatial variation ($g(x)\approx g(0)$, short stack approximation, $\ell << 2\pi c_0/\omega$),

$$\frac{\partial}{\partial x}\left[g(x)\frac{\partial\theta}{\partial x}\right] = g\frac{\partial^2\theta}{\partial x^2}. \tag{21}$$

Finally Eq. (18) becomes, for $x\in(0,\ell)$,

$$\frac{\partial\theta}{\partial t} = g\frac{\partial^2\theta}{\partial x^2}-\zeta_L\theta+q_v. \tag{22}$$

In the right hand side of Eq. (22), it can be noted that the first term represents the effect of the conductive heat flux returning inside the stack enhanced by the acoustically induced thermal conductivity (see expression (15) of $g(x)$), whereas the second term accounts for the heat leakages through the lateral duct wall and the third term for the heat generated by viscous losses inside the stack enhanced by the non-uniformity of the thermoacoustic process along the stack.

At each boundary of the stack, $x=0$ and $x=\ell$, the conductive heat flux which crosses from the inside to the outside of the stack per unit area and per unit time is balanced by both the heat transfer towards the heat exchangers through the end of the stack (with a heat-transfer coefficient $h_{e_{0,\ell}}$), and the heat flux reaching the end of the stack, which is the combination of the thermoacoustic heat flux Q_{th} given by Eq. (5) and a heat flux Q_{vort} which represents a possible additional heating due to non-linear phenomena at the ends of the stack associated with high levels of velocity (vorticity and minor losses at the ends of the stack [32], for example)

$$K_{eq}\frac{\partial\theta}{\partial x}-h_{e_0}\theta = Q_{th}(0)-Q_{vort}(0), \quad x=0,\ t>0, \tag{23a}$$

$$K_{eq}\frac{\partial\theta}{\partial x}+h_{e_\ell}\theta = Q_{th}(\ell)+Q_{vort}(\ell), \quad x=\ell,\ t>0, \tag{23b}$$

where $h_{e_{0,\ell}}$ denotes an empirical heat exchange coefficient and where Q_{vort} is an empirical phenomenological coefficient. Finally, the homogeneous boundary-value problem for the stack is governed by Eq. (22) in the interval $x\in(0,\ell)$, by the boundary conditions at $x=0$ and $x=\ell$ given by Eqs. (23a) and (23b) and by the initial condition, leading to the following one-dimensional set of fundamental equations of heat conduction for the transient temperature distribution inside the stack:

$$\frac{1}{g}\frac{\partial\theta}{\partial t} = \frac{\partial^2\theta}{\partial x^2}-\alpha\theta+\beta, \quad x\in(0,\ell),\ t>0, \tag{24a}$$

$$\frac{\partial\theta}{\partial x}-\eta_0\theta = q_0, \quad x=0,\ t>0, \tag{24b}$$

$$\frac{\partial\theta}{\partial x}+\eta_\ell\theta = q_\ell, \quad x=\ell,\ t>0, \tag{24c}$$

$$\theta(x,0) = \varphi(x), \quad x\in(0,\ell),\ t=0, \tag{24d}$$

where $\alpha=\zeta_L/g, \beta=q_v/g,\ \eta_{0,\ell}=h_{e_{0,\ell}}/[K_{eq}+r],\ q_0=[q(0)-Q_{vort}(0)]/[K_{eq}+r],\ q_\ell=[q(\ell)+Q_{vort}(\ell)][q(\ell)+Q_{vort}(\ell)][K_{eq}+r],\ q(0)$ and $q(\ell)$ being given by Eq. (6), q_v being considered uniform along the stack (short stack approximation) and the function $\varphi(x)$ accounting for the initial temperature spatial distribution.

Solution of this problem for the transient temperature distribution along the x-axis inside the stack as a function of the time, assuming short stack approximation (g, α and β assumed to be constant), when the acoustic energy is provided to the thermoacoustic resonator from time $t=0$, is achieved with the aid of an expansion which involves the normal mode functions of the associated eigenvalue problem. The details of the derivation are given in the next section.

3. The modal solution for the temperature profile

The relevant boundary eigenvalue problem for an ordinary differential equation, which is associated to the problem as posed above and which can be easily solved providing a set of orthogonal eigenfunctions (here Fourier series), takes the form of the system of equations

$$\left(\frac{\partial^2}{\partial x^2}+k_m^2\right)\psi_m(x)=0,\quad x\in(0,\ell), \tag{25a}$$

$$\left(\frac{\partial}{\partial x}-\eta_0\right)\psi_m(x)=0,\quad x=0, \tag{25b}$$

$$\left(\frac{\partial}{\partial x}+\eta_\ell\right)\psi_m(x)=0,\quad x=\ell. \tag{25c}$$

The solution which obeys this system of equations is found to have the explicit form [30]

$$\psi_m(x)=N_m^{-1}[k_m\cos(k_m x)+\eta_0\sin(k_m x)], \tag{26a}$$

with

$$N_m^2=\frac{1}{2}\left[\left(k_m^2+\eta_0^2\right)\left(\ell+\frac{\eta_\ell}{k_m^2+\eta_\ell^2}\right)+\eta_0\right], \tag{26b}$$

so that the eigenfunctions ψ_m are normalized, i.e.

$$\int_0^\ell \psi_{m_1}\psi_{m_2}dx=\delta_{m_1 m_2}. \tag{26c}$$

The eigenvalues k_m are solutions of the equation

$$\tan(k_m\ell)=\frac{k_m(\eta_0+\eta_\ell)}{k_m^2-\eta_0\eta_\ell}. \tag{26d}$$

To determine the temperature profile, one introduces the expansion

$$\theta=\sum_{m=0}^{\infty}C_m(t)\psi_m(x), \tag{27}$$

where the individual coefficient functions $C_m(t)$ are given by

$$C_m(t)=\int_0^\ell \psi_m(x)\theta(x,t)dx, \tag{28a}$$

denotes below

$$C_m(t)=\langle\psi_m|\theta\rangle. \tag{28b}$$

These coefficient functions $<\psi_m|\theta>$ are subsequently found from multiplying the diffusion Eq. (24a) by the eigenfunction ψ_m and integrating over the interval $(0,\ell)$. It follows

$$\frac{1}{g}\frac{\partial}{\partial t}\langle\psi_m|\theta\rangle=\left\langle\psi_m\left|\frac{\partial^2}{\partial x^2}\theta\right.\right\rangle-\alpha\langle\psi_m|\theta\rangle+\langle\psi_m|\beta\rangle, \tag{29a}$$

and, with the aid of the Green theorem,

$$\left[\frac{1}{g}\frac{\partial}{\partial t}+\alpha\right]\langle\psi_m|\theta\rangle=\left\langle\frac{\partial^2}{\partial x^2}\psi_m\left|\theta\right.\right\rangle+\left[\psi_m\frac{\partial}{\partial x}\theta-\theta\frac{\partial}{\partial x}\psi_m\right]_0^\ell+\langle\psi_m|\beta\rangle. \tag{29b}$$

Then, invoking Eq. (25a), the coefficients $C_m(t)$ are solution of

$$\left[\frac{\partial}{\partial t}+g(k_m^2+\alpha)\right]C_m(t)=f_m(t), \tag{30a}$$

where

$$f_m(t)=g[q_\ell\psi_m(\ell)-q_0\psi_m(0)+\langle\psi_m|\beta\rangle]. \tag{30b}$$

Accounting for the initial condition (24d), the solution of Eq. (30a) is given by

$$C_m(t)=e^{-g\left(k_m^2+\alpha\right)t}\left\{\langle\psi_m|\varphi(x)\rangle+\int_0^t e^{g\left(k_m^2+\alpha\right)t_0}f_m(t_0)dt_0\right\}. \tag{31}$$

Finally, assuming that the function $f_m(t_0)$ does not depends significantly on time, and that the initial condition $\varphi(x)$ is here equal to zero, the solution is thus explicitly given by

$$\theta=-\sum_m(q_\ell\psi_m(\ell)-q_0\psi_m(0)+\langle\psi_m|\beta\rangle)\left[\frac{e^{-g\left(k_m^2+\alpha\right)t}-1}{\left(k_m^2+\alpha\right)}\right]\psi_m(x), \tag{32a}$$

with, in the frame of the "short stack" approximation (β does not depend on the coordinate x),

$$\langle\psi_m|\beta\rangle=N_m^{-1}\beta\left[\sin(k_m\ell)+\frac{\eta_0}{k_m}(1-\cos(k_m\ell))\right]. \tag{32b}$$

Further simplifications, assuming namely that the heat leakages through the lateral duct wall and towards resonator are neglected, and that the heat generated by viscous losses inside the stack is not taken into account, lead directly to the results discussed by previous authors [9]. According to these simplifications, if one allows the parameters η_0, η_ℓ, ζ_L and β to shrink to zero, the solution (32a) takes the form [5]

$$\theta=(q_\ell+q_0)\sqrt{\frac{2}{\ell}}\sum_{m\ \ odd}\left[1-e^{-gk_m^2t}\right]\frac{1}{k_m^2}\sqrt{\frac{2}{\ell}}\cos k_m x,\quad k_m=\frac{m\pi}{\ell}, \tag{33a}$$

where the first summation represents a linear contribution to the temperature distribution inside the stack, namely,

$$\sum_{m\ \ odd}\left(\frac{\ell}{m\pi}\right)^2\sqrt{\frac{2}{\ell}}\cos\left(\frac{m\pi}{\ell}x\right)=-\frac{1}{2}\sqrt{\frac{\ell}{2}}\left(x-\frac{\ell}{2}\right). \tag{33b}$$

It must be noticed that this theoretical temperature distribution does not fit correctly with the experimental results. The discussion presented in the next section lies on result (32) and does not assume these last approximations.

Remark: In the formulation presented above (set of Eqs. (24a)–(24d)) it is assumed that the heat transfers towards each part of the resonator through the ends $x=0$ and $x=\ell$ of the stack depend only on the temperature difference θ (involving empirical heat exchange coefficients in Eqs. (24b) and (24c)). Another approach (Appendix A) can be built on a classical model for these heat transfers which includes both the diffusion process inside each part of the thermoacoustic resonator and the heat flux between each ends of the stack and heat exchangers (set at $x=0$ and $x=\ell$, respectively). A suitable analytical solution for the temperature difference θ can be obtained in the Fourier domain and the solution in the time domain can then be expressed using Cauchy's theorem in the complex plane. However, it is necessary to assume appropriate approximations to give analytical expressions. Namely, the heat leakages through the ends of the stack have to be neglected. In other words, the solution can be formally analytic, although its actual implementation involves unavoidable numerical calculations.

4. Analytical and experimental results

4.1. Experimental setup and results

A view of the thermoacoustic refrigerator used for experiments is shown in Fig. 2. This device consists of a half-wavelength resonator with a constant square cross section (length $L+x_0=86$ cm;

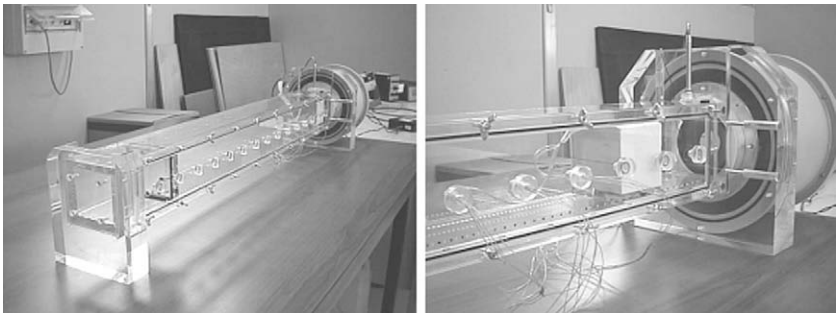

Fig. 2. Experimental setup.

Table 1
Fitted values of empirical parameters for three stack positions.

Stack centre position x_c (cm)	h_{e_0} (W m^{-2} K^{-1})	h_{e_ℓ} (W m^{-2} K^{-1})	Q_{vort} (W m^2)
72	30	30	0
62	72	42	56
43	75	80	272

section $S = 80 \times 80$ mm^2), closed by a rigid wall at one end and coupled to an electrodynamic loudspeaker (Focal 4V3211) at the other end. This resonator is filled with air at atmospheric pressure and at ambient temperature.

The thermoacoustic core is not a stack of parallel plates, but a ceramic porous material made of cordierite which is usually used in catalytic exhaust pipe. This ceramic, called stack in the following, contains a multitude of square cross section channels (600 CPSI, length $\ell = 60$ mm, transversal width $2y_0 = 0.92$ mm, wall thickness $2e_s = 0.12$ mm) parallel to the resonator axis. This stack can be set at any position in the resonator. Note that this prototype does not comprise any heat exchanger. The thermo-physical and geometrical characteristics of the prototype are summarised in Table 1. Temperature measurements are carried out along the stack by the use of thirteen type K thermocouples (127 μm in diameter) equally spaced along the median axis of the stack (each 5 mm). An additional type K thermocouple is set on the external wall of the resonator in order to monitor the ambient temperature during the measurements. The acoustic pressure is measured by a microphone flush-mounted on the wall at the entrance of the resonator (near the membrane of the loudspeaker). During experiments, the working frequency is tuned at the first resonance of the device, that is $f \approx 200$ Hz, and the amplitude of the acoustic pressure at the entrance of the resonator is set at $p_0 = 1500$ Pa.

The time evolution of the temperature along the stack axis is measured during the transient process for three different positions of the stack in the resonator (defined by the abscissa x_c of the stack centre) as shown in Fig. 3. This evolution is shown in Fig. 4 for a position of the stack which leads to an experimentally maximal

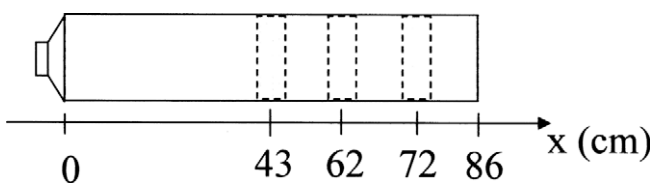

Fig. 3. Schematic view of the cylindrical thermoacoustic refrigerator and the three different positions of the stack in the resonator.

temperature difference ΔT between the ends of the stack. This optimal position depends on the frequency, on the shape and the dimensions of the stack, on the thermo-physical properties of the fluid and the plates, and on the acoustic pressure level in the resonator [33]. For this device, the optimal position of the stack centre is either $x_c = 18.5$ cm or $x_c = 72$ cm (symmetrical positions about the half length of the resonator). The results given on Fig. 4 are obtained at the position $x_c = 72$ cm. Before switching on the loudspeaker, the system is at thermal equilibrium, the temperature distribution along the stack being uniform ($T_m = 28$ °C, Fig. 4(c), curve denoted t_1) and the temperature difference ΔT between the ends of the stack being then equal to zero. During the first seconds after switching on the loudspeaker, the temperature at the end of the stack closest to the loudspeaker decreases, while the temperature at the opposite end increases (Fig. 4(a)). The temperature profile along the stack is then symmetrically bending at the stack ends, while it remains constant at the middle of the stack (Fig. 4(c), curve denoted t_2). After a while, the temperature gradient along the stack becomes almost uniform (Fig. 4(c), curve denoted t_3). Then, about 500 s after switching on the loudspeaker, the steady state temperature difference ΔT between the ends of the stack is reached ($\Delta T = 12$ °C, Fig. 4(b)). Nevertheless, the temperature profile is not symmetrical about the uniform temperature distribution at rest: each thermocouple along the stack undergoes a small thermal drift towards higher temperature (around 1 °C about 900 s after switching on the loudspeaker as shown in Fig. 4(c), curve denoted t_4).

Fig. 5 shows the evolution of the temperature along the stack axis for a stack centre set at the mid-length of the resonator ($x_c = 43$ cm). For this position, each thermocouple along the stack undergoes almost the same heating (no cooling is observed), and the temperature difference ΔT obtained between the two ends of the stack is very small (about 1.2°C, Fig. 5(b)). About 10 min after switching on the loudspeaker, the thermal drift experienced by each thermocouple along the stack is around 3.5 °C (Fig. 5(c), curve denoted t_4).

Fig. 6 shows the evolution of the temperature along the stack axis for a stack centre set in the resonator at a distance $x_c = 62$ cm from the loudspeaker. This intermediate position between the optimal position and the mid-length of the resonator approximately corresponds to the median position between a pressure node and a pressure antinode in the resonator. The temperature difference ΔT between the two ends of the stack reaches its steady state value ($\Delta T \approx 8$ °C, Fig. 6(b)) about 400 s after switching on the loudspeaker. Each thermocouple along the stack undergoes the same thermal drift towards higher temperature. This drift is more important than the drift experienced at optimal position (around 2.7 °C about 900 s after switching on the loudspeaker). After a while, the temperature of the cold end of the stack comes back to its rest value.

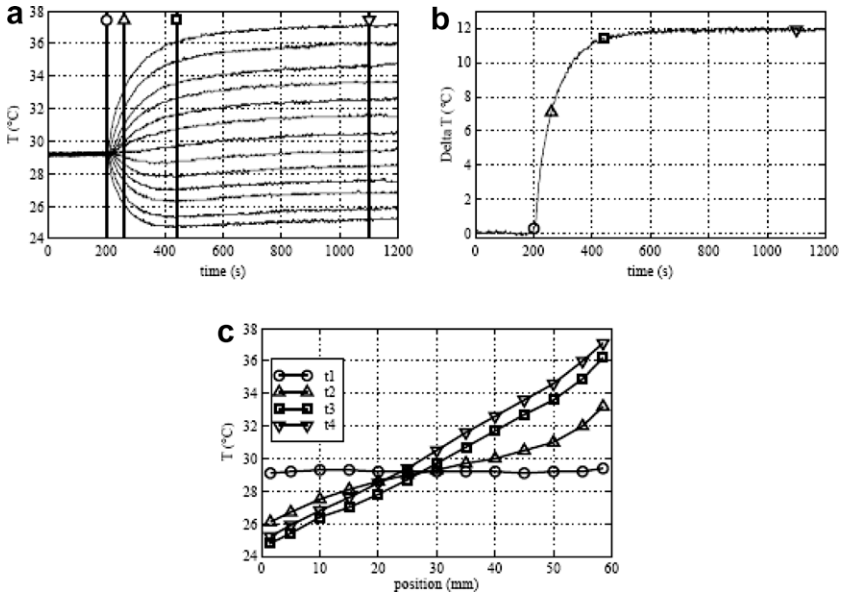

Fig. 4. Experimental time evolution of the mean temperature for a position of the stack centre $x_c = 72$ cm. (a) Time evolution of the mean temperature of thirteen points regularly distributed along the axis of the stack. (b) Time evolution of temperature difference between the two ends of the stack. (c) Time evolution of the mean temperature distribution along the axis of the stack: t_1 is the time when switching on the loudspeaker (○), t_2 is 60 s after switching on the loudspeaker (△), t_3 is 240 s after switching on the loudspeaker (□), and t_4 is 900 s after switching on the loudspeaker (▽).

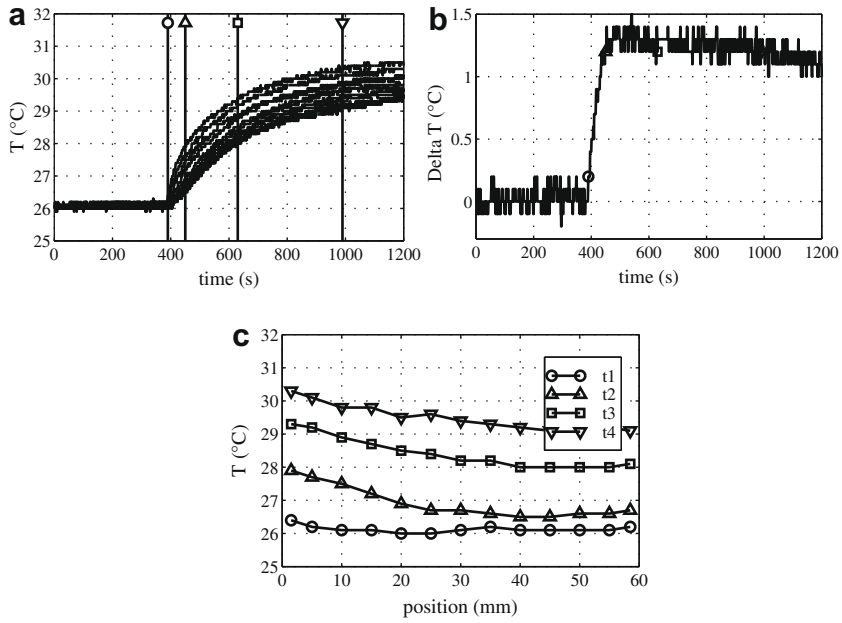

Fig. 5. Experimental time evolution of the mean temperature for a position of the stack centre in the resonator $x_c = 43$ cm. (a) Time evolution of the mean temperature of thirteen points regularly distributed along the axis of the stack. (b) Time evolution of temperature difference between the two ends of the stack. (c) Time evolution of the mean temperature distribution along the axis of the stack: t_1 is the time when switching on the loudspeaker (○), t_2 is 60 s after switching on the loudspeaker (△), t_3 is 240 s after switching on the loudspeaker (□), and t_4 is 600 s after switching on the loudspeaker (▽).

4.2. Analytical results

The different behaviours observed on the experimental results can be obtained by the use of the analytical modelling presented in Sections 2 and 3. Analytical results and experimental data are reported on Figs. 7–9 for the three different positions of the stack in the resonator. Figs. 7(a), 8(a) and 9(a) give the theoretical (full lines) and experimental (doted lines) time evolutions of the temperatures of two points located inside the stack at 10 mm far from each end, respectively, avoiding then edge effects. Figs. 7(b), 8(b) and 9(b) give the theoretical (full lines) and experimental (doted lines) time evolutions of the temperature difference between these two points. Figs. 7(c), 8(c) and 9(c) give the theoretical (full lines) and experimental (doted lines) time evolutions of the temperature distribution along the stack. The concordance between experimental and analytical temperature time evolutions is obtained by fitting the values of several empirical parameters: h_L, $h_{e_{0,\ell}}$ and Q_{vort} (see Table 1). First, the value of heat exchange coefficient h_L is here chosen to be very low (<1) because the stack is laterally well thermally isolated. Second, the heat exchange coefficients h_{e_0} and h_{e_ℓ} are considered as empirical in an interval compatible with the approximate results given in the literature (see below). Third, the heat flux Q_{vort} due to

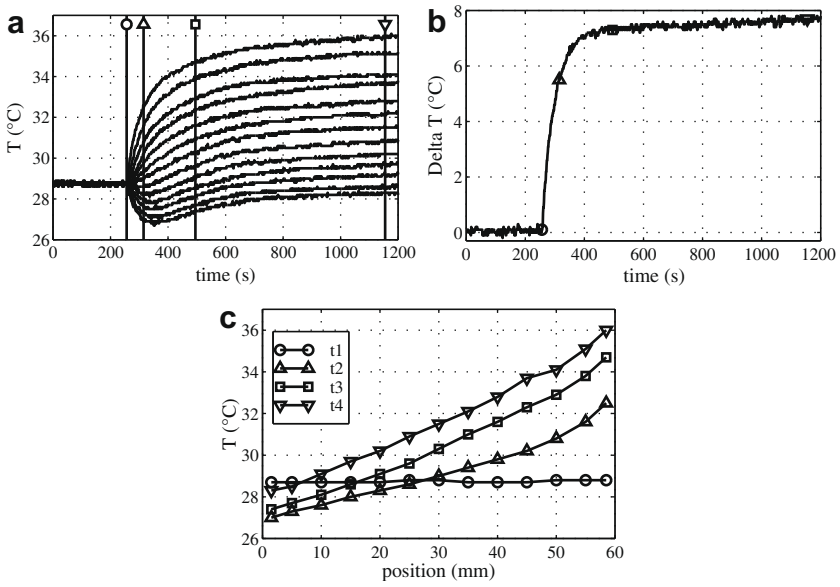

Fig. 6. Experimental time evolution of the mean temperature for a position of the stack centre in the resonator $x_c = 62$ cm. (a) Time evolution of the mean temperature of thirteen points regularly distributed along the axis of the stack. (b) Time evolution of temperature difference between the two ends of the stack. (c) Time evolution of the mean temperature distribution along the axis of the stack: t_1 is the time when switching on the loudspeaker $(\circ)$, t_2 is 60 s after switching on the loudspeaker $(\triangle)$, t_3 is 240 s after switching on the loudspeaker $(\square)$, and t_4 is 900 s after switching on the loudspeaker (∇).

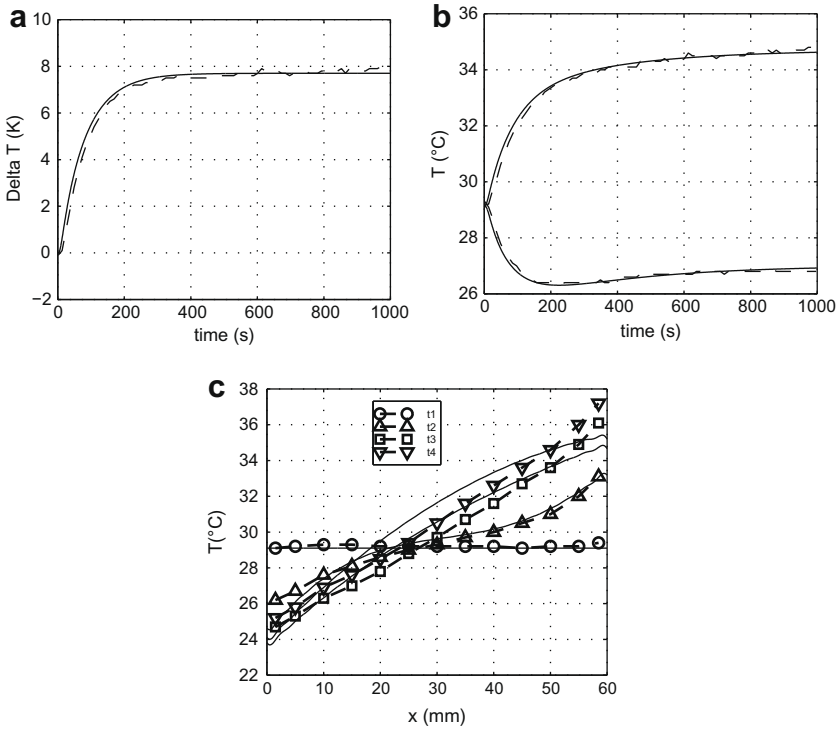

Fig. 7. Theoretical (full lines) and experimental (dotted lines) time evolution of the mean temperature for a position of the stack centre in the resonator $x_c = 72$ cm. (a) Time evolution of the mean temperature of two points located inside the stack at 10 mm far from each end, respectively. (b) Time evolution of temperature difference between these two points. (c) Time evolution of the mean temperature distribution along the axis of the stack: t_1 is the time when switching on the loudspeaker $(\circ)$, t_2 is 60 s after switching on the loudspeaker $(\triangle)$, t_3 is 240 s after switching on the loudspeaker $(\square)$, and t_4 is 900 s after switching on the loudspeaker (∇).

vorticity at the ends of the stack is considered as a phenomenological parameter, the theoretical evaluation of Q_{vort} having yet to be worked out. The identification of both heat exchange coefficients and vorticity heat flux is achieved simultaneously with the Levenberg–Marquard method, using the "lsqnonlin" Matlab routine. Note that the value of the heat Q_v generated by viscous losses inside the stack is assumed here to be equal to twice the value given by the Eq. (10), taking then into account the fact that the stack used in experimental setup is a set of parallel square ducts.

When the stack centre is set at its optimal position in the resonator ($x_c = 72$ cm), the concordance between experimental and analytical results is achieved with $h_{e_0} = 30\ \mathrm{W\,m^{-2}\,K^{-1}}$, $h_{e_\ell} = 30$

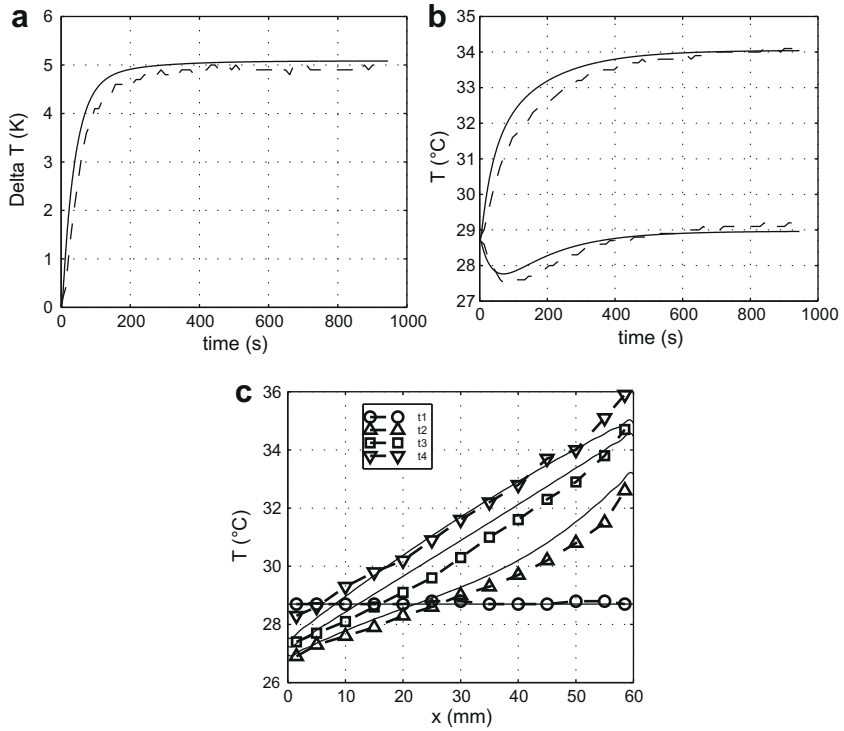

Fig. 8. Theoretical (full lines) and experimental (dotted lines) time evolution of the mean temperature for a position of the stack centre in the resonator $x_c = 62$ cm. (a) Time evolution of the mean temperature of two points located inside the stack at 10 mm far from each end, respectively. (b) Time evolution of temperature difference between these two points. (c) Time evolution of the mean temperature distribution along the axis of the stack: t_1 is the time when switching on the loudspeaker $(\circ)$, t_2 is 60 s after switching on the loudspeaker $(\triangle)$, t_3 is 240 s after switching on the loudspeaker $(\square)$, and t_4 is 900 s after switching on the loudspeaker (∇).

W m^{-2} K^{-1} and $Q_{vort} = 0$. When the stack centre is set at the intermediate position between the optimal position and the mid-length of the resonator ($x_c = 62$ cm), the concordance between experimental and analytical results is achieved with $h_{e_0} = 72$ W m^{-2} K^{-1}, $h_{e_\ell} = 42$ W m^{-2} K^{-1} and $Q_{vort} = 56$ W m^{-2}. When the stack centre is set at the mid-length of the resonator ($x_c = 43$ cm), the concor-

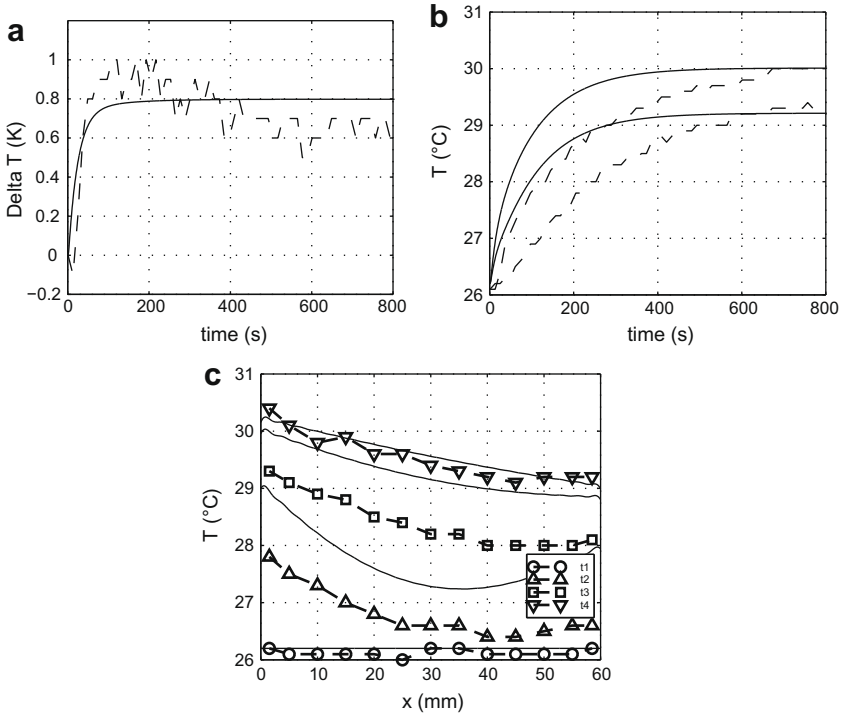

Fig. 9. Theoretical (full lines) and experimental (dotted lines) time evolution of the mean temperature for a position of the stack centre in the resonator $x_c = 43$ cm. (a) Time evolution of the mean temperature of two points located inside the stack at 10 mm far from each end, respectively. (b) Time evolution of temperature difference between these two points. (c) Time evolution of the mean temperature distribution along the axis of the stack: t_1 is the time when switching on the loudspeaker $(\circ)$, t_2 is 60 s after switching on the loudspeaker $(\triangle)$, t_3 is 240 s after switching on the loudspeaker $(\square)$, and t_4 is 600 s after switching on the loudspeaker (∇).

dance between experimental and analytical results is achieved with $h_{e_0} = 75\ \mathrm{W\,m^{-2}\,K^{-1}}$, $h_{e_\ell} = 80\ \mathrm{W\,m^{-2}\,K^{-1}}$ and $Q_{vort} = 272\ \mathrm{W\,m^{-2}}$.

The fitted values of heat exchange coefficients $h_{e_{0,\ell}}$ and the fitted value of heat due to vorticity Q_{vort} depend on the position of the stack in the resonator: they are increasing when the stack is moved toward the resonator centre. This behaviour is not surprising since the amplitude of the particle velocity is increasing in the same way. The fitted values of heat exchange coefficients $h_{e_{0,\ell}}$ have the expected order of magnitude of heat exchange coefficients reported in the literature for such geometry in oscillating flows [34,35]. Actually, the adjustment of these empirical parameters prevents us to derive results with sufficiently accurate precision to obtain very fine quantitative conclusions. Forthcoming works have yet to be conducted in order to derive theoretical estimations of these parameters. Nevertheless, the reasonable good quantitative agreement between analytical and experimental results allows the interpretation of the transient behaviour as follows. The discussion is limited here to the case of the intermediate position between the optimal position and the mid-length of the resonator (Fig. 8), because it offers the advantage of clearly showing the effects of the different phenomena taken into account in the theoretical model. At the beginning of the process, during the first seconds following the start of the loudspeaker, the temperature at the end of the stack closest to the loudspeaker decreases whilst the temperature at the opposite end increases (Fig. 8(a)): that is the effect of the thermoacoustic heat flux Q_{th} reaching the ends of the stack. After few hundreds of seconds, the temperature difference between the ends of the stack tends toward a limit (Fig. 8(b)), the thermoacoustic heat flux being balanced by the conductive heat flux Q_c returning in the stack region, enhanced by the effect of the thermoacoustically induced thermal conductivity r. The effect of both the heat Q_ν generated by viscous losses inside the stack and the heat Q_{vort} generated at the ends of the stack leads to a global heating of the stack. This effect coexists with the thermoacoustic effect, but predominates once thermoacoustic effect is balanced with heat conduction. Then, the temperature of each point of the stack increases (the temperature of the "cold end" reaching again its initial value), and finally tends towards a limit value (Fig. 8(a)) due to heat transfer through the ends of the stack.

5. Conclusion

In conclusion, this paper provides the first complete yet simple model to describe the transient behaviour of the temperature profile in the stack of classical thermoacoustic refrigerators. The experimental results have provided confirmation of the theoretical prediction showing more particularly the specific shape of the curves (especially the shape at the beginning of the transient) and thus the characteristic times of the transient, emphasising that each effect which occurs plays an important role in the transient profile of the temperature inside the stack. Moreover, the agreement between the experimental and theoretical values of the stationary temperature difference between the ends of the stack shows that the model presented in this paper conveys an interpretation of the physical phenomena, namely the role played by the thermoacoustic heat flux carried along the stack, the conductive heat flux returning in the solid walls of the stack and through the fluid inside the stack, the transverse heat conduction in the stack and heat leakages through the duct walls, heat generated by viscous losses in the stack and minor losses at the ends of the stack, and heat transfer through both ends of the stack.

The results presented in this paper convey our conviction that the analytical model would provide accurate description of the transient of classical thermoacoustic devices. It is worth noting that the sensitivity of the theoretical results to the value of the parameters is quite important (the fitted values of the parameters are always obtained with a precision which reach roughly 1%), but because these parameters are unknown (only their orders of magnitude can be obtained from data available in the literature), this prevents us from validating quantitatively the theory. Presumably, the theoretical method presented in this paper will be adequate to access the precise value of such parameters in non-stationary regime with a good precision. These kind of measurements, lying on this method, and their validations have yet to be worked out.

Acknowledgement

The authors would like to acknowledge the Direction Générale de l'Armement (DGA) and the Agence Nationale de la Recherche (ANR, MicroThermAc Project) for financial support.

Appendix A. Basic equations and solutions for the temperature difference between the ends of the stack (Fourier transform)

In the formulation presented in Section 2 (set of Eqs. (24a)–(24d)) it is assumed that the heat transfers towards the heat exchangers through the ends $x = 0$ and $x = \ell$ of the stack depend only on the temperature difference θ (involving empirical heat exchange coefficients, Eqs. (24b) and (24c)). The approach shortly described in the remark at the end of Section 3 is built on a classical model for these heat transfers when heat exchangers are considered as heat sinks. This model includes both the diffusion process inside the parts $i = 1$ and 3 of the thermoacoustic resonator (Fig. 10), and the heat flux between each ends of the stack and heat exchangers (set at $x = 0$ and $x = \ell$, respectively). Then, Eqs. (24b) and (24c) are replaced by the set of four equations

$$-K_{eq}\frac{\partial\theta(0)}{\partial x} + K_1\frac{\partial\theta_1(0)}{\partial x} - \left(q(0) + r(0)\frac{\partial\theta(0)}{\partial x}\right) = C_0\frac{\partial\theta_0}{\partial t}, \quad x = 0,\ t > 0, \tag{34}$$

$$K_{eq}\frac{\partial\theta(\ell)}{\partial x} - K_3\frac{\partial\theta_1(\ell)}{\partial x} + \left(q(\ell) + r(\ell)\frac{\partial\theta(\ell)}{\partial x}\right) = C_\ell\frac{\partial\theta_\ell}{\partial t}, \quad x = \ell,\ t > 0, \tag{35}$$

$$\frac{\partial\theta_1}{\partial t} = g_1\frac{\partial^2\theta_1}{\partial x^2} - \zeta_1\theta_1, \quad x \leqslant 0,\ t > 0, \tag{36}$$

$$\frac{\partial\theta_3}{\partial t} = g_3\frac{\partial^2\theta_3}{\partial x^2} - \zeta_3\theta_3, \quad x \geqslant \ell,\ t > 0, \tag{37}$$

where θ, θ_1, θ_3, θ_0 and θ_ℓ denote the temperature difference $(T_m - T_\infty)$ between the mean temperature T_m inside the thermoacoustic resonator and T_∞ the ambient temperature outside the resonator, respectively, in the stack, in the parts of the reonator denoted 1 and 3 and in the heat exchangers located, respectively, at $x = 0$ and $x = \ell$, where C_0 and C_ℓ are the heat capacity of the heat exchangers, and K_1 and K_3 are the diffusive thermal conductivity of

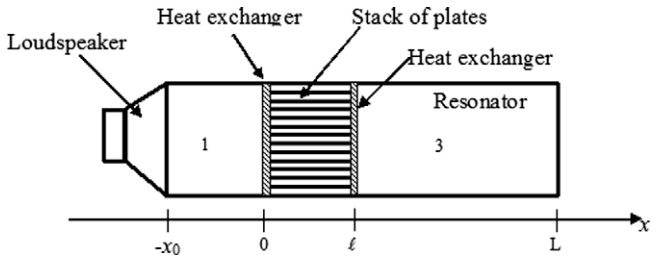

Fig. 10. Schematic view of the cylindrical thermoacoustic refrigerator with heat exchangers.

the fluid in the resonator (the other notations being given in the text), with the interface conditions

$$\theta(0) = \theta_1(0) = \theta_c \tag{38}$$

and

$$\theta(\ell) = \theta_3(\ell) = \theta_h \tag{39}$$

while Eqs. (24a) and (24d) remain valid:

$$\frac{\partial\theta}{\partial t} = g\frac{\partial^2\theta}{\partial x^2} - \zeta_L\theta + q_v, \quad x \in (0,\ell), \ \ t > 0, \tag{40}$$

$$\theta(x,0) = 0, \quad x \in (0,\ell), \ \ t = 0. \tag{41}$$

The suitable analytical solution for the temperature difference θ inside the stack can be expressed in the Fourier domain, and then in the time domain using Cauchy's theorem. However, it would be necessary to assume appropriate approximations to give tractable analytical expressions, namely the heat leakages through the ends of the stack have to be neglected (which is a limit of the method).

Appendix B. Parameters and their values used in the numerical calculations and in the experimental device

Notation	Definition	Unity	Numerical value
Geometrical parameters (resonator and stack)			
$L + x_0$	Resonator length	m	86×10^{-2}
S	Resonator section area	m^2	0.8×0.8
ℓ	Stack length	m	6×10^{-2}
$2e_s$	Stack-plate thickness	m	0.12×10^{-3}
$2y_0$	Fluid layer thickness	m	0.92×10^{-3}
Thermo-physical parameters of the stack plates			
C_s	Specific heat coefficient per unit of mass	$J\,kg^{-1}\,K^{-1}$	1000
K_s	Thermal conductivity	$W\,m^{-1}\,K^{-1}$	0.19
ρ_S	Density	$kg\,m^{-3}$	1.4×10^3
Thermo-physical properties of the working gas			
ρ_0	Density	$kg\,m^{-3}$	1.2
c_0	Adiabatic speed of sound	$m\,s^{-1}$	344
K	Thermal conductivity	$W\,m^{-1}\,K^{-1}$	2.55×10^{-2}
C_p	Specific heat coefficient per unit of mass	$J\,kg^{-1}\,K^{-1}$	1004
μ	Shear viscosity coefficient	$kg\,m^{-1}\,s^{-1}$	1.82×10^{-5}
P_0	Atmospheric pressure	Pa	1.013×10^5

References

[1] G. Swift, Thermoacoustic engines, J. Acoust. Soc. Am. 84 (1988) 1145–1180.
[2] L. Yaoyu, M. Rotea, L. Mongeau, P. In-Su, Extremum seeking control of a tunable thermoacoustic cooler, IEEE Trans. Control Syst. Technol. 13 (2005) 527–536.
[3] J. Vargasa, I. Horuzb, T. Callenderc, J. Flemming, J. Parisee, Simulation of the transient response of heat driven refrigerators with continuous temperature control, Int. J. Refrig. 21 (1998) 648–660.
[4] T. Pfafferott, G. Schmitz, Modelling and transient simulation of CO_2-refrigeration systems with modelica, Int. J. refrig. 27 (2004) 42–52.
[5] S. Duffourd, Réfrigérateur thermoacoustique: études analytique et expérimentales en vue d'une miniaturisation – miniaturisation of thermoacoustic refrigerator: analytical and experimental studies, Ph.D. thesis, Ecole Centrale de Lyon, 2001.
[6] A. Piccolo, G. Cannistraro, Convective heat transport along a thermoacoustic couple in the transient regime, Int. J. Therm. Sci. 41 (2002) 1067–1075.
[7] D. Marx, P. Blanc-Benon, Numerical simulation of stack–heat exchangers coupling in a thermoacoustic refrigerator, AIAA J. 42 (2004) 1338–1347.
[8] D. Marx, P. Blanc-Benon, Numerical simulation of the temperature difference between the extremities of a thermoacoustic stack plate, Cryogenics 45 (2005) 163–172.
[9] R.T. Muehleisen, A.A. Atchley, Simple model for temperature gradient formation in a short stack, J. Acoust. Soc. Am. 103 (1998) 2840.
[10] L. Bauwens, Thermoacoustics: transient regimes and singular temperature profiles, Phys. Fluids 10 (1998) 807–818.
[11] G. Swift, Analysis and performance of a large thermoacoustic engine, J. Acoust. Soc. Am. 92 (1992) 1151–1563.
[12] V. Müller, E. Lang, Experimente mit thermisch getriebenen gasflüssigheits-schwingungen, J. Appl. Math. Phys. (ZAMP) 36 (1985).
[13] J. Olson, G. Swift, Acoustic streaming in pulse tube refrigerators: tapered pulse tubes, Cryogenics 37 (1997) 769–776.
[14] J. Wheatley, T. Hofler, G. Swift, A. Migliori, Understanding of simple phenomena in thermoacoustics with applications to acoustic heat engines, Am. J. Phys. 53 (1985) 147–162.
[15] V. Gusev, H. Bailliet, P. Lotton, M. Bruneau, Asymptotic theory of nonlinear acoustic waves in a thermoacoustic prime-mover, Acust. – Acta Acust. 86 (2000) 25–38.
[16] G. Penelet, E. Gaviot, V. Gusev, P. Lotton, M. Bruneau, Experimental investigation of transient nonlinear phenomena in an annular thermoacoustic prime-mover: observation of a double-threshold effect, Cryogenics 42 (2002) 527–532.
[17] G. Penelet, V. Gusev, P. Lotton, M. Bruneau, Nontrivial influence of acoustic streaming on the efficiency of annular thermoacoustic prime movers, Phys. Lett. A 351 (2006) 268–273.
[18] A.A. Atchley, T.J. Hofler, M.L. Muzzerall, M.D. Kite, C. Ao, Acoustically generated temperature gradients in short plates, J. Acoust. Soc. Am. 88 (1990) 251–263.
[19] M. Wetzel, C. Herman, Design optimization of thermoacoustic refrigerators, Internat. J. Refrig. 20 (1997) 3–21.
[20] A.S. Worlikar, O. Knio, R. Klein, Numerical simulation of a thermoacoustic refrigerator. Part 2: Stratified flow around the stack, J. Comp. Phys. 144 (1998) 299–324.
[21] Y.T. Kim, S.J. Suh, M.G. Kim, Linear resonant duct thermoacoustic refrigerator having regenerator stacks, in: Proceedings of the 16th International Congress on Acoustics, 1998.
[22] A.A. Atchley, H.E. Bass, T.J. Hofler, Development of nonlinear waves in a thermoacoustic prime mover, in: Frontiers of nonlinear acoustics: 12th ISNA, 1990.
[23] V. Gusev, P. Lotton, H. Bailliet, S. Job, M. Bruneau, Thermal wave harmonics generation in the hydrodynamical heat transport in thermoacoustics, J. Acoust. Soc. Am. 109 (2001) 84–90.
[24] G. Mozurkewich, Time-average distribution in a thermoacoustic stack, J. Acoust. Soc. Am. 103 (1998) 380–388.
[25] V. Gusev, P. Lotton, H. Bailliet, S. Job, M. Bruneau, Relaxation time approximation for analytical evaluation of temperature field in thermoacoustic stack, J. Sound Vib. 235 (2000) 1338–1347.
[26] S. Karpov, A. Prosperetti, A nonlinear model of thermoacoustic devices, J. Acoust. Soc. Am. 112 (2002) 1431–1444.
[27] M.F. Hamilton, Y.A. Ilinskii, E.A. Zabolotskaya, Nonlinear two-dimensional model for thermoacoustic engines, J. Acoust. Soc. Am. 111 (2002) 2076–2086.
[28] D. Marx, P. Blanc-Benon, Computation of the temperature distorsion in the stack of a standing-wave thermoacoustic refrigerator, J. Acoust. Soc. Am. 118 (2005) 2993–2999.
[29] H. Bailliet, P. Lotton, M. Bruneau, V. Gusev, Coupling between loudspeakers and thermoacoustic cavities, Acta Acust. 86 (2000) 363–373.
[30] M.N. Ozizik, Heat Conduction, John Wiley and Sons Inc., 1993.
[31] H.S. Carslaw, J.C. Jaeger, Conduction of Heat in Solids, Clarendon Press, Oxford, 1997.
[32] M. Mironov, V. Gusev, Y. Auregan, P. Lotton, M. Bruneau, P. Piatakov, Acoustic streaming related to minor loss phenomenon in differentially heated elements of thermoacoustically devices, J. Acoust. Soc. Am. 112 (2002) 441–445.
[33] G. Poignand, B. Lihoreau, P. Lotton, E. Gaviot, M. Bruneau, V. Gusev, Optimal acoustic fields in compact thermoacoustic refrigerators, Appl. Acoust. 68 (2007) 642–659.
[34] A. Piccolo, G. Pistone, Estimation of heat transfer coefficients in oscillating flows: the thermoacoustic case, Int. J. Heat Mass Transfer 49 (2006) 1631–1642.
[35] J.R. Brewster, R. Raspet, H.E. Bass, Temperature discontinuities between elements of thermoacoustic devices, J. Acoust. Soc. Am. 102 (1997) 3355–3360.